Available online at www.sciencedirect.com

ScienceDirect

Ceramics International 39 (2013) 8701–8708

CERAMICS INTERNATIONAL

www.elsevier.com/locate/ceramint

Phase transition, microstructure and electrical properties of Fe doped $Ba_{0.70}Ca_{0.30}TiO_3$ lead-free piezoelectric ceramics

Cai-Xia Li[a,b], Bin Yang[a,*], Shan-Tao Zhang[c,*], Rui Zhang[a], Ye Sun[a], Jun-Jun Wang[a], Rui-Xue Wang[a], Wen-Wu Cao[a,d]

[a]Department of Physics, Condensed Matter Science and Technology Institute, Harbin Institute of Technology, Harbin 150001, PR China
[b]Department of Materials and Physics, School of Applied Sciences, Harbin University of Science and Technology, Harbin 150080, PR China
[c]Department of Materials Science and Engineering & National Laboratory of Solid State Microstructures, Nanjing University, Nanjing 210093, PR China
[d]Materials Research Institute, The Pennsylvania State University, University Park, PA 16802, USA

Received 27 February 2013; received in revised form 3 April 2013; accepted 15 April 2013
Available online 21 April 2013

Abstract

Lead-free piezoelectric ceramics of $Ba_{0.70}Ca_{0.30}Ti_{1-x}Fe_xO_3$ ($x=0$–0.03) have been synthesized by a conventional solid state reaction method. The influence of Fe content on the microstructure, phase transition, dielectric, ferroelectric, and piezoelectric properties is investigated systematically. The ceramics with $x\leq0.02$ are diphasic composites of tetragonal $Ba_{0.80}Ca_{0.20}TiO_3$:Fe and orthorhombic $Ba_{0.07}Ca_{0.93}TiO_3$:Fe solid solutions. The tetragonal phase is gradually suppressed as x increases, the ceramic with $x=0.03$ is found to have diphasic pseudocubic and orthorhombic phases. And the grain size is dependent on Fe content significantly. Introduction of Fe at B-sites improves the densification and decreases the sintering temperature. As x increases from 0 to 0.03, the room temperature relative dielectric permittivity enhances, dielectric loss decreases, and the Curie temperature decreases monotonically from 128 °C to 58 °C. However, the ferroelectricity enhances slightly and reaches the maximum near $x=0.005$, and then weakens with increasing x. On the other hand, the piezoelectric coefficient (d_{33}) and the electromechanical coupling coefficient (k_p) decrease simultaneously with increasing x, whereas the mechanical quality factor (Q_m) increases significantly. The structure–electrical properties relationship is discussed intensively to give more information on (Ba,Ca)TiO_3-based lead-free piezoelectric ceramics.

Keywords: C. Piezoelectric properties; $Ba_{0.70}Ca_{0.30}Ti_{1-x}Fe_xO_3$; Phase transition; Microstructure

1. Introduction

As one of the most important perovskite-type ferroelectric materials, $BaTiO_3$ (BT) and BT-based materials show promising dielectric, piezoelectric and electrostrictive properties [1–3], which have been of practical interest in various applications, such as multilayered ceramic capacitors (MLCC), piezoelectric devices, optoelectronic element, and semiconductors [4]. Extensive research work has been carried out on BT-based solid solutions to improve the dielectric, ferroelectric and piezoelectric properties [5–7]. Among the modified BT-based materials, $(1-x)BaTiO_3$–$xCaTiO_3$ (BCTx) solid solutions have received considerable attention as a lead-free piezoelectric material [2,6,8–10]. In BCTx solid solutions, the partial substitution of Ba^{2+} by Ca^{2+} causes a negligible change of the Curie temperature (T_C), but a strong decrease of the tetragonal–orthorhombic phase transition temperature (T_{O-T}), which leads to improved temperature reliability of the tetragonal phase, and inhibited formation of the undesired hexagonal phase of BT. It is noticed that there is a solubility limit for Ca^{2+} substituting for Ba^{2+} around x=0.23, above which, both tetragonal and orthorhombic phases coexist within the range of $0.23<x<0.90$ [4,11,12].

It has been known that composite and diphasic materials may possess the potential capability of performing far beyond those of constituent materials because of the enhanced properties, which are generally attributed to the coupling between two equivalent energy states [11,13,14]. For example, diphasic

*Corresponding authors. Tel.: +86 13836127592/+86 13951976481.
E-mail addresses: binyang@hit.edu.cn (B. Yang), stzhang@nju.edu.cn (S.-T. Zhang).

0272-8842/$ - see front matter © 2013 Elsevier Ltd and Techna Group S.r.l. All rights reserved.
http://dx.doi.org/10.1016/j.ceramint.2013.04.052

BCTx ceramics near the solubility limit show larger electrostrictive strain (ES), and higher ferroelectric and piezoelectric properties than the pure ferroelectric tetragonal phase of BCTx, this observation is attributed to the interaction between the ferroelectric tetragonal phase and the dielectric orthorhombic phase [1]. Furthermore, high ES, strong electroluminescence (EL) and mechanoluminescence (ML) are obtained simultaneously in BCTx:Pr ceramics near the solubility limit in the diphasic region, and it is suggested that the interactions of the large ionic polarization in orthorhombic phase with the domains in tetragonal phase play an important role in improving ES properties and creating new ML and EL features in BCTx:Pr ceramics [15]. And additionally, high piezoelectric properties (d_{33}~361 pC/N, k_p~41.2%) in $(Ba_{0.94}Ca_{0.02})Ti_{0.94}O_{\delta}$–0.04LiF ceramics are observed and ascribed to the coexistence of orthorhombic and pseudocubic phases [16]. Recently, based on the diphasic $Ba_{0.70}Ca_{0.30}TiO_3$, several lead-free piezoelectric ceramics with a high piezoelectric performance have been developed [2,8–10], which usually possess a triple point in the phase diagram. However, these ceramics are usually sintered at relatively high temperature (1450–1500 °C), which restricts their practical applications.

Therefore, preparing high performance BCT-based ceramics with low sintering temperature is important and interesting. Such work on BT has been carried out and several processing approaches have been explored, such as doping with different dopants at A and B sites [7,16], microwave sintering [17], two-step sintering [18], and reducing particle size of the raw materials [19,20]. Among them, doping with different dopants at A and B sites is an effective and easily controllable method [21]. Substitution of both isovalent and aliovalent cations for the host ions in the perovskite lattice sites would produce point defect such as vacancies, which can help promote atomic diffusion during sintering. For example, it is reported that introduction of CuO could improve the densification process, decrease the sintering temperature and enhance electrical properties of BT [7]. However, it should be noticed that although the influence of introduction of various dopants in BT-based ceramics has been investigated [21–24], no detailed studies about the effects of dopants on the physical properties of $Ba_{0.70}Ca_{0.30}TiO_3$ have been reported, which have drawn considerable attentions as described above.

On the other hand, it is reported that addition of Fe_2O_3 into $BaTiO_3$ [25], and $Bi_{0.5}Na_{0.5}TiO_3$ [26] could lead to higher density, lower sintering temperature, and modified properties. Accordingly, to improve sintering ability and obtain higher electrical performance, in this paper we prepared $Ba_{0.70}Ca_{0.30}Ti_{1-x}Fe_xO_3$ (x=0–0.03) lead-free piezoelectric ceramics, and investigated the influence of Fe content on the microstructure, phase transition, dielectric, ferroelectric, and piezoelectric properties. The structure–electrical properties were discussed intensively.

2. Experimental procedure

$Ba_{0.70}Ca_{0.30}Ti_{1-x}Fe_xO_3$ ceramics (x=0, 0.002, 0.005, 0.01, 0.015, 0.02 and 0.03) were fabricated by a conventional solid-state reaction method with the raw materials of $BaCO_3$ (99.0%), $CaCO_3$ (99.0%), TiO_2 (99.0%), and Fe_2O_3 (99.99%). The powders were mixed and ball-milled in alcohol for 24 h using agate balls in a planetary mill, the slurry was dried, and then calcined at 950 °C for 3 h. The calcined powders were ball milled again for 24 h, dried, and then pressed into disks of 13 mm in diameter and 0.5–1.0 mm in thickness under 80 MPa using 8 wt% polyvinyl alcohol (PVA) as a binder, which was burnt out by slow heating at 550 °C for 2 h. Sintering was conducted between 1250 °C and 1270 °C in air for 2 h, lower sintering temperature for compositions with higher Fe content. The bulk densities were obtained by the Archimedes method. All the samples had relative densities higher than 95%.

The phases of ceramics were checked by X-ray powder diffraction (XRD, D/max 2400: Rigaku Inc. D, Japan) on an automated Rigaku D/max 2400 X-ray diffractometer with rotating anode using CuKα radiation. The microstructures were observed by a back-scattered scanning electron microscopy (SEM, Quanta 200FEG system: FEI. Co. USA) with X-ray energy dispersive spectroscopy (EDS) for chemical analysis. The ceramics were polished carefully and painted with silver pastes on both surfaces of the pellets and fired at 600 °C for 30 min. Dielectric properties were measured upon heating from −80 °C to 180 °C at 0.1–100 kHz using a programmable furnace with an Agilent 4284A LCR meter. Ferroelectric hysteresis (P–E) loops and bipolar strain–electric field (S–E) curves were measured at room temperature at 1 Hz using a ferroelectric tester (Radiant Technologies, Inc, Albuquerque, NM) in silicone oil. The samples were poled with the field of 30 kV/cm for 20 min at room temperature in a silicone oil bath. The piezoelectric constant d_{33} was measured using a quasi-static d_{33} testing meter (ZJ-4A, Institute of Acoustics, Chinese Academy of Sciences, Beijing, China). The planar electromechanical coupling coefficient k_p and the mechanical quality factor Q_m were determined by a resonance–antiresonance method using an precision impedance analyzer (4294A, Agilent Technologies, Hewlett-Packard, Palo Alto, CA) and calculated following IEEE standards.

3. Results and discussion

Fig. 1 shows the room temperature XRD patterns of the $Ba_{0.70}Ca_{0.30}Ti_{1-x}Fe_xO_3$ ceramics (x=0, 0.002, 0.005, 0.01,

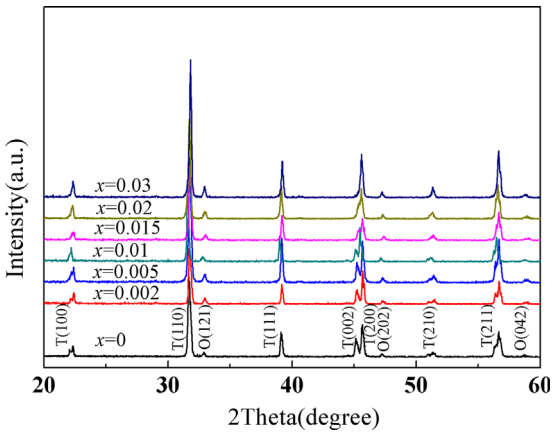

Fig. 1. XRD patterns of $Ba_{0.70}Ca_{0.30}Ti_{1-x}Fe_xO_3$ ceramics (x=0–0.03).

0.015, 0.02 and 0.03). All the ceramics possess a perovskite structure without any trace of impurity phases. The tetragonal symmetry is characterized by the splitting of (002)/(200) peaks at 2θ—46° and the existence of a single (111) peak at 2θ—40° [27], suggesting that the ceramics with $x \leq 0.02$ are in diphasic coexistence and composed of tetragonal $Ba_{0.80}Ca_{0.20}TiO_3$:Fe solid solution and orthorhombic $Ba_{0.07}Ca_{0.93}TiO_3$:Fe solid solution, in agreement with early reports [1,11,12]. With increasing Fe content, the tetragonal structure gradually diminishes and the (002) peak steadily becomes weak, and completely merges with the (200) peak at $x=0.03$, indicating that the phase structure of the $Ba_{0.70}Ca_{0.30}Ti_{1-x}Fe_xO_3$ ceramics evolves from the tetragonal–orthorhombic phases coexistence to pseudocubic–orthorhombic diphasic phases.

Fig. 2 shows the back-scattered field emission SEM micrographs of the $Ba_{0.70}Ca_{0.30}Ti_{1-x}Fe_xO_3$ ceramics sintered at 1270 °C for 2 h with different Fe contents ($0 \leq x \leq 0.03$), and the EDS observations show that all the ceramics have well developed grain morphologies with improved densification, the small orthorhombic $Ba_{0.07}Ca_{0.93}TiO_3$:Fe grains (black grains) disperse among the larger tetragonal $Ba_{0.80}Ca_{0.20}TiO_3$:Fe grains matrix (white grains), consistent with the diphasic composite structure composed of the tetragonal $Ba_{0.80}Ca_{0.20}TiO_3$:Fe and orthorhombic $Ba_{0.07}Ca_{0.93}TiO_3$:Fe

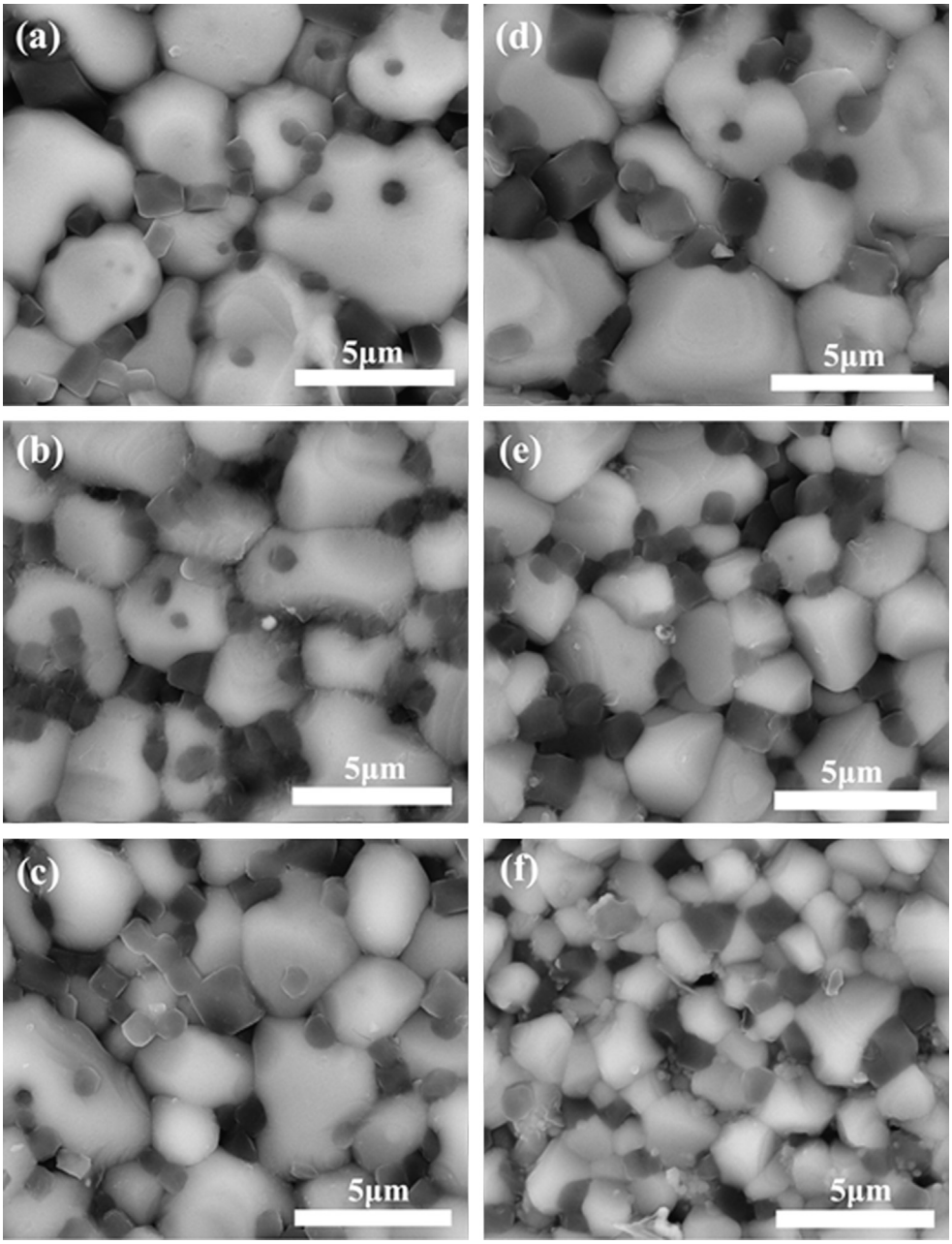

Fig. 2. SEM micrographs of $Ba_{0.70}Ca_{0.30}Ti_{1-x}Fe_xO_3$ ceramics sintered at 1270 °C for 2 h (a) $x=0.002$, (b) $x=0.005$, (c) $x=0.01$, (d) $x=0.015$, (e) $x=0.02$ and (f) $x=0.03$.

solid solution for $Ba_{0.70}Ca_{0.30}Ti_{1-x}Fe_xO_3$ ceramics shown in the XRD data and consistent with early reports [1,11,15]. The grain sizes of the tetragonal and orthorhombic phases are shown in Table 1; as can be seen, the grain size of the tetragonal phase increases first, reaches the maximum of 5.45 μm at $x=0.005$, and then decreases with increasing x, while that of the orthorhombic phase shows a slight increase monotonically. The relative densities are 95.4%, 96.0%, 96.4%, 96.5%, 96.7%, and 96.8% for the compositions with $x=0.002$, 0.005, 0.01, 0.015, 0.02 and 0.03 respectively. As x increases, the relative density of the ceramics increases, confirming that the introduction of Fe improves the densification of $Ba_{0.70}Ca_{0.30}TiO_3$ ceramics, which may have resulted from the substitution of Ti by Fe cations, for the ionic radius of Fe^{3+} (0.645 Å) is closer to the ionic radius of Ti^{4+} (0.68 Å) than that of Ba^{2+} (1.34 Å) and Ca^{2+} (0.99 Å), so Fe cations may preferentially substitute Ti cations. Moreover, the ratio of cationic radius to anionic radius (O^{2-}, 1.40 Å) would exclude the Fe ion from residing at the Ba or Ca site due to the instability of the structure [26], therefore, oxygen vacancies may appear to compensate the charge imbalance arising from the substitution of B-sites by Fe^{3+}, the amount of oxygen vacancies increase with the increasing amount of Fe^{3+} ions substituting Ti sites, which helps promote atomic diffusion during sintering to improve densification of ceramics.

Table 1
Grain size of $Ba_{0.70}Ca_{0.30}Ti_{1-x}Fe_xO_3$ ceramics.

Fe content x	Grain size (T) (μm)	Grain size (O) (μm)
0.002	5.34	0.96
0.005	5.45	0.96
0.010	4.49	0.97
0.015	4.22	1.28
0.020	3.21	1.52
0.030	2.26	1.53

The temperature dependence of the relative dielectric constant and the dielectric loss for $Ba_{0.70}Ca_{0.30}Ti_{1-x}Fe_xO_3$ ceramics at 10 kHz is shown in Fig. 3(a) and (b), respectively. As can be seen, the tetragonal–cubic phase transition (T_C) can be observed for all the ceramics in the range of measurement temperature, and

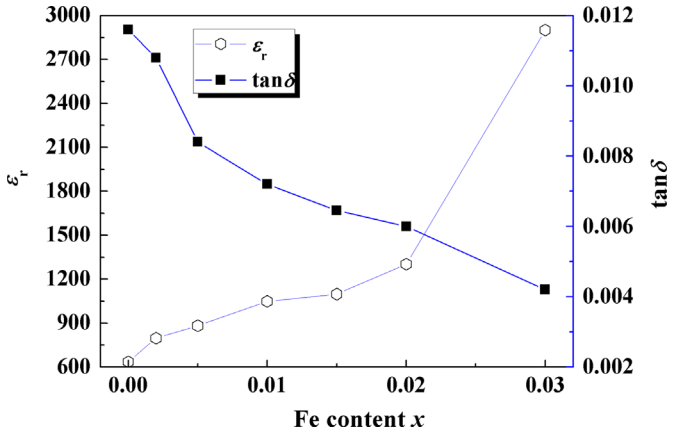

Fig. 4. Room temperature relative dielectric constant and dielectric loss of $Ba_{0.70}Ca_{0.30}Ti_{1-x}Fe_xO_3$ ceramics as functions of Fe content at 1 kHz.

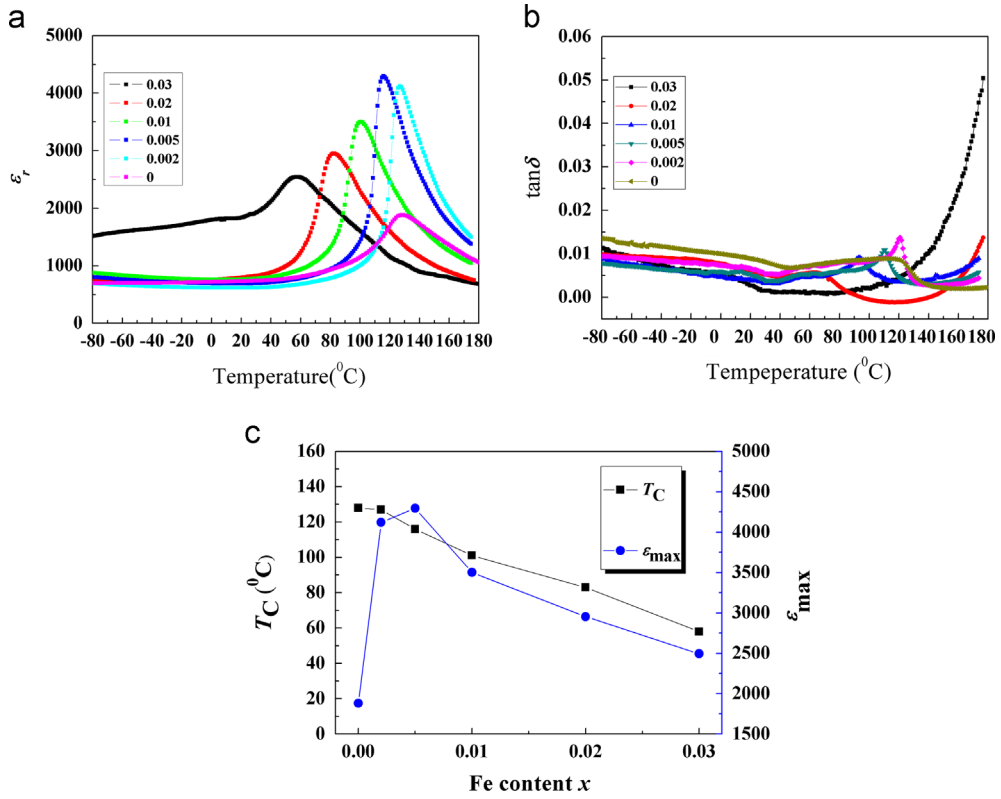

Fig. 3. Temperature dependence of (a) relative dielectric constant, (b) dielectric loss for $Ba_{0.70}Ca_{0.30}Ti_{1-x}Fe_xO_3$ ceramics at 10 kHz, and (c) T_C and ε_{max} of $Ba_{0.70}Ca_{0.30}Ti_{1-x}Fe_xO_3$ ceramics as functions of Fe content.

T_C decreases monotonically from 128 °C to 58 °C as x increases from 0 to 0.03, while the dielectric maximum (ε_{max}) reaches the maximum at $x=0.005$ and then decreases, as plotted in Fig.3(c). The relative dielectric constant at 1 kHz at room temperature increases significantly from 635 for pure $Ba_{0.70}Ca_{0.30}TiO_3$ up to 2901 for the composition with $x=0.03$, and the dielectric loss decreases monotonically from 0.012 to 0.004 as x increases from 0 to 0.03 as shown in Fig. 4, which may be due to the denser microstructure caused by the introduction of Fe and the decreased T_C toward room temperature as increasing Fe content.

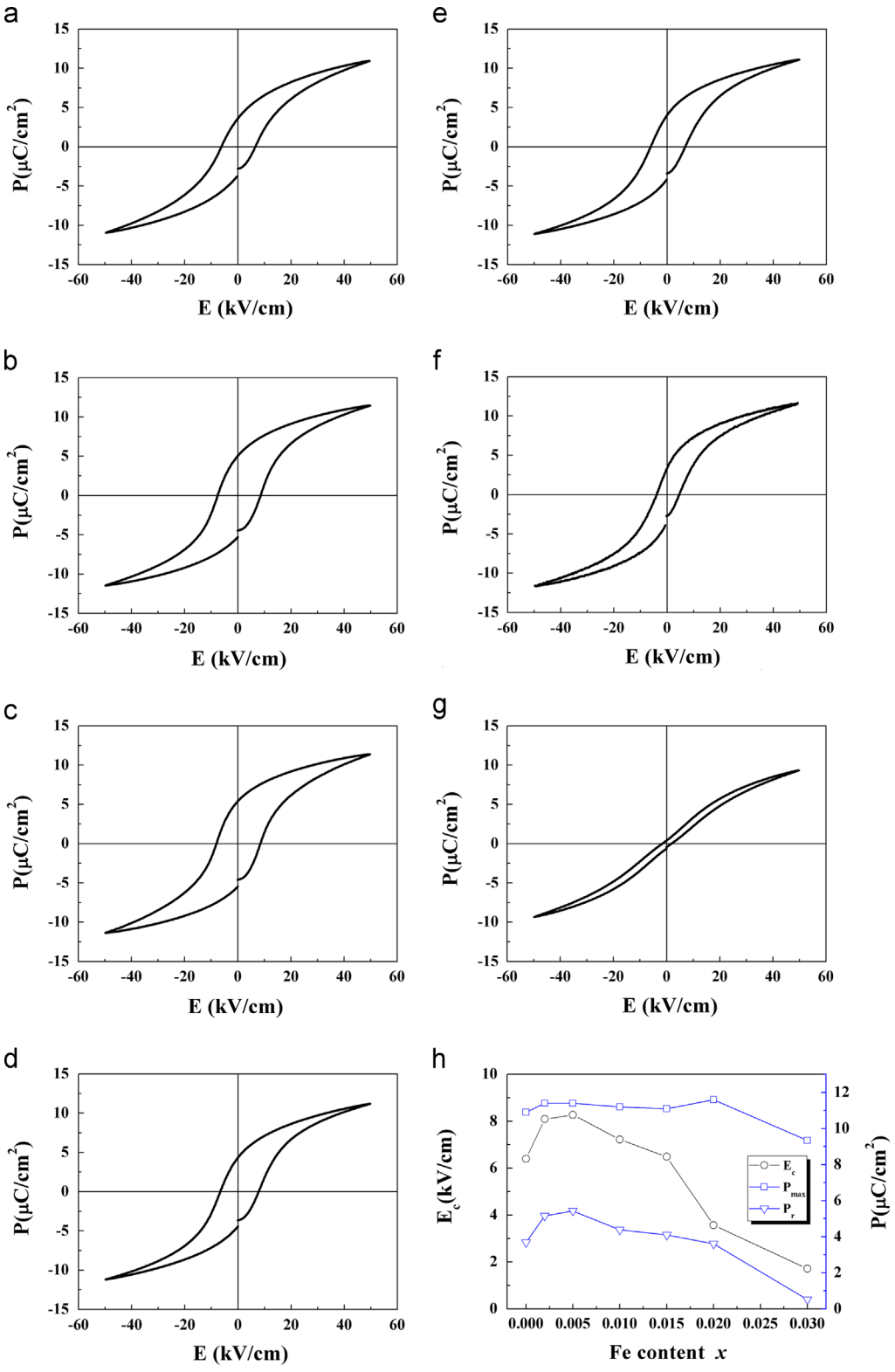

Fig. 5. Room temperature P–E hysteresis loops of $Ba_{0.70}Ca_{0.30}Ti_{1-x}Fe_xO_3$ ceramics with (a) $x=0$, (b) $x=0.002$, (c) $x=0.005$, (d) $x=0.01$, (e) $x=0.015$, (f) $x=0.02$, (g) $x=0.03$, and (h) P_{max}, P_r, and E_c values of $Ba_{0.70}Ca_{0.30}Ti_{1-x}Fe_xO_3$ ceramics as functions of Fe content.

Fig. 5(a)–(g) shows the polarization–electric field (*P–E*) hysteresis loops of the $Ba_{0.70}Ca_{0.30}Ti_{1-x}Fe_xO_3$ ceramics measured at room temperature. All samples possess a typical ferroelectric polarization hysteresis loop. Fig. 5(h) plots the variation of maximum polarization (P_{max}), remnant polarization (P_r) and coercive field (E_c) of the $Ba_{0.70}Ca_{0.30}Ti_{1-x}Fe_xO_3$ ceramics against the Fe content. It can be seen that as x increases, these parameters first increase slowly, reach the maximum near $x=0.005$, and then decrease remarkably to 9.3 μC/cm^2, 0.5 μC/cm^2, and 1.7 kV/cm for P_{max}, P_r, and E_c respectively for the ceramics with $x=0.03$. The sample with $x=0.005$ shows the maximum P_r of 5.4 μC/cm^2 with a corresponding E_c of 8.3 kV/cm, which may be attributed to the pinning effect of domain walls caused by the increase of oxygen vacancies generated by the substitution of Fe^{3+} for Ti^{4+}. Moreover, the increased grain size of the tetragonal phase by the introduction of Fe cations for the ceramics with $x=0.005$ is positive for ferroelectric property, because it is suggested that small grain size means large amount of grain boundary, and ground boundary will lead to polarization discontinuity between grains and hence decreased polarization [28]. However, the P_{max}, P_r, and E_c values decrease simultaneously with further increasing x, which may be due to the suppressed tetragonal phase and enhanced pseudocubic phase caused by addition of Fe.

The bipolar strain–electric field (*S–E*) hysteresis loops of the $Ba_{0.70}Ca_{0.30}Ti_{1-x}Fe_xO_3$ ceramics at room temperature are shown in Fig. 6. All ceramics exhibit butterfly-shaped *S–E* curves, which are typical for ferroelectric materials. As Fe content increases from 0 to 0.005, the strain loops show a more typical ferroelectric behavior, which is evident from the enhancement of the maximum strain and negative strain (the difference between the zero field strain and the lowest strain which is only visible in the bipolar cycle). Maximum strains of 0.14% and 0.15% were observed for the ceramics with $x=0.002$ and 0.005 respectively. And then with further increasing x, the maximum strain gradually decreases while the negative strain nearly vanishes. The composition dependence of *S–E* curves is consistent with that of the *P–E* loops. It is suggested that some interaction exists between the diphasic phases composed of ferroelectric tetragonal $Ba_{0.80}Ca_{0.20}TiO_3$:Fe solid solution and normal dielectric orthorhombic $Ba_{0.07}Ca_{0.93}TiO_3$:Fe solid solution [1,11]. A large strain is believed to originate from the non-180° domain rotation driven by an external electric field [1]. In the composite $Ba_{0.70}Ca_{0.30}Ti_{1-x}Fe_xO_3$ ceramics ($x=0$–0.02), $Ba_{0.07}Ca_{0.93}TiO_3$:Fe grains disperse among the ceramics, their large ionic polarization couples with the non-180° domains in surrounding ferroelectric tetragonal $Ba_{0.80}Ca_{0.20}TiO_3$:Fe grains. The polarization enhances the polarizability and domain rotation ability of the ceramics during the external electric field exertion [1]. Moreover, the increased grain size of the tetragonal phase by Fe doping for the ceramics with $x\leq0.005$ is positive for ferroelectric property. The above effects should be responsible for the observed increased strain by Fe doping when $x\leq0.005$. On the other hand, as a "hard" dopant, the substitution of Fe for Ti will create oxygen vacancies to compensate the charge imbalance, which will usually reduce the strain of the piezoceramics. When $x\leq0.005$, the positive effect dominates, whereas when $x\geq0.005$, the detrimental effect tends to be dominative.

Fig. 7 shows the piezoelectric coefficient (d_{33}), the planar mode electromechanical coupling coefficient (k_p), and the mechanical quality factor (Q_m) as functions of Fe content for the $Ba_{0.70}Ca_{0.30}Ti_{1-x}Fe_xO_3$ ceramics. It is observed that the d_{33}

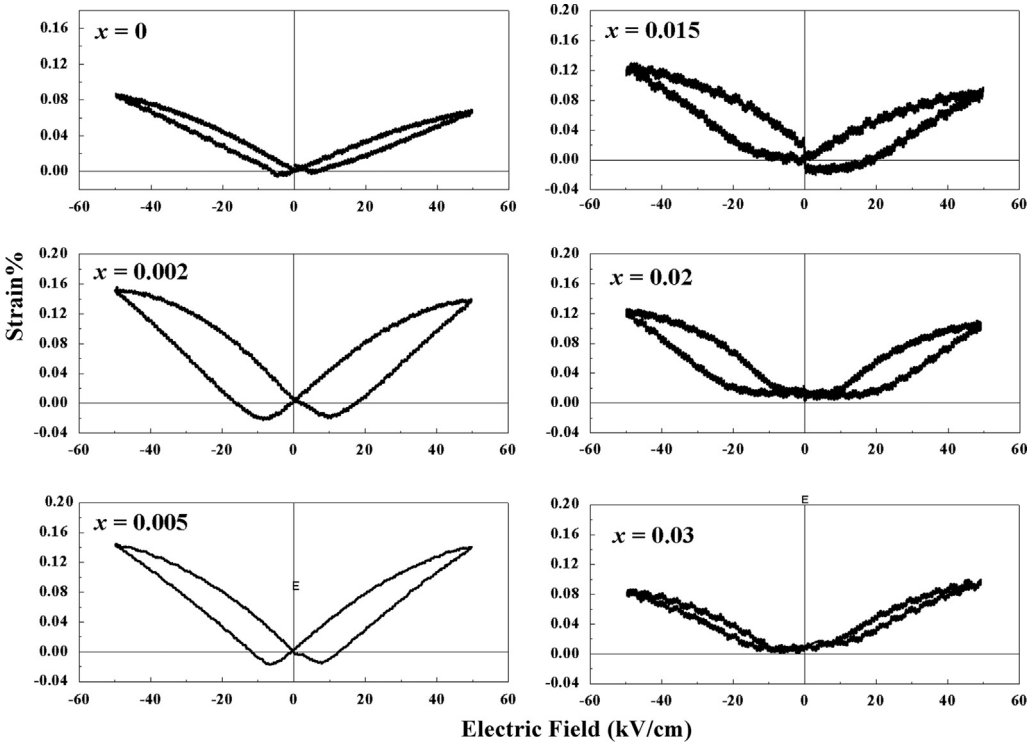

Fig. 6. Bipolar *S–E* curves of $Ba_{0.70}Ca_{0.30}Ti_{1-x}Fe_xO_3$ ceramics ($x=0$–0.03).

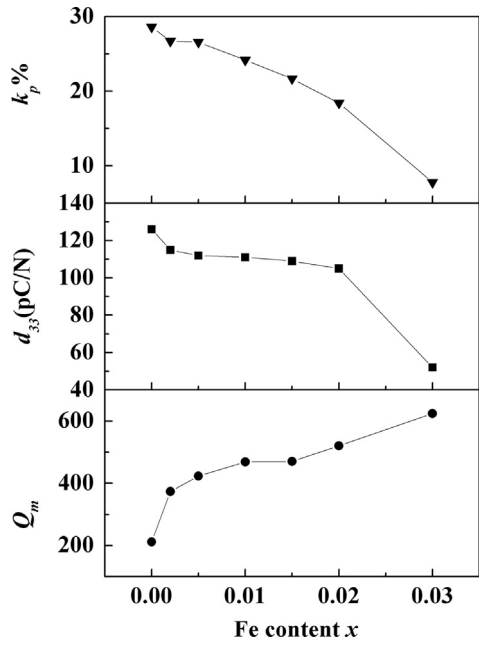

Fig. 7. d_{33}, k_p, and Q_m values of the $Ba_{0.70}Ca_{0.30}Ti_{1-x}Fe_xO_3$ ceramics as functions of Fe content.

and k_p show a similar decreasing tendency as x increases, which may be ascribed to the phase transition from tetragonal to pseudocubic symmetry and the ferroelectric–paraelectric phase transition temperature is decreased to near room temperature with increasing x, whereas the mechanical quality factor (Q_m) increases significantly with increasing x, which may have resulted from the interaction from the diphasic phases in the ceramics.

4. Conclusions

$Ba_{0.70}Ca_{0.30}Ti_{1-x}Fe_xO_3$ lead-free piezoelectric ceramics ($x=0$–0.03) have been prepared. The influence of Fe content on the microstructure, phase transition, density, and electrical properties is investigated. The ceramics with $x\leq0.02$ are diphasic composites of tetragonal $Ba_{0.80}Ca_{0.20}TiO_3$:Fe and orthorhombic $Ba_{0.07}Ca_{0.93}TiO_3$:Fe solid solutions; an increase of Fe content suppresses the tetragonal phase and enhances the pseudocubic phase, as a result, the ceramics with $x=0.03$ have coexisted pseudocubic and orthorhombic phases. Obviously composition dependent grain size is observed. Introduction of Fe at B-sites improves the densification and decreases the sintering temperature, which can be ascribed to the promoted atomic diffusion during sintering by the increase of oxygen vacancies, which is generated by the substitution of Fe^{3+} for Ti^{4+}. As x increases from 0 to 0.03, the room temperature relative dielectric permittivity enhances, dielectric loss decreases, and the Curie point decreases monotonically from 128 °C to 58 °C, however, the ferroelectric properties show a maximum with $x=0.005$, and then weaken with further increasing x. The structure–ferroelectric and piezoelectric properties relationship is discussed intensively to supply more information for understanding BCT-based lead-free piezoelectric ceramics.

Acknowledgments

This work was supported by the Key Technologies R&D Program of China under (Grant no. 2013BAI03B06), the National Science and Technology Support Program (SQ2012BAJY3766), the National Key Basic Research Program of China (973 Program, 2013CB632900), the National Nature Science Foundation of China (10704021, 51102062, and 11174127), and the Key Scientific and Technological Project of Harbin (Grant no. 2009AA3BS131).

References

[1] X.S. Wang, H. Yamada, C.N. Xu, Large electrostriction near the solubility limit in $BaTiO_3$–$CaTiO_3$ ceramics, Applied Physics Letters 86 (2005) 022905.
[2] D.Z. Xue, Y.M. Zhou, H.X. Bao, J.H Gao, C. Zhou, X.B. Ren, Large piezoelectric effect in Pb-free $Ba(Ti,Sn)O_3$–$x(Ba,Ca)TiO_3$ ceramics, Applied Physics Letters 99 (2011) 122901.
[3] L.J. Liu, S.Y. Zheng, Y.M. Huang, D.P. Shi, S.S Wu, L. Fang, C.Z. Hu, B. Elouadi, Structure and piezoelectric properties of $(1-0.5x)BaTiO_3$–$0.5x(0.4BaZrO_3$–$0.6CaTiO_3)$ ceramics, Journal of Physics D: Applied Physics 45 (2012) 295403.
[4] B. Jaffe, W.R. Cook, H. Jaffe, Piezoelectric Ceramics, Academic Press, London, 1971.
[5] N. Ma, B.P. Zhang, W.G. Yang, D. Guo, Phase structure and nano-domain in high performance of $BaTiO_3$ piezoelectric ceramics, Journal of the European Ceramic Society 32 (2012) 1059–1066.
[6] P. Wang, Y.X. Li, Y.Q. Lu, Enhanced piezoelectric properties of $(Ba_{0.85}Ca_{0.15})(Ti_{0.9}Zr_{0.1})O_3$ lead-free ceramics by optimizing calcination and sintering temperature, Journal of the European Ceramic Society 31 (2011) 2005–2012.
[7] P. Zheng, J.L. Zhang, S.F. Shao, Y.Q. Tan, C.L. Wang, Piezoelectric properties and stabilities of CuO-modified $Ba(Ti,Zr)O_3$ ceramics, Applied Physics Letters 94 (2009) 032902.
[8] D.Z. Xue, Y.M. Zhou, H.X. Bao, C. Zhou, J.H. Gao, X.B. Ren, Elastic, piezoelectric, and dielectric properties of $Ba(Zr_{0.2}Ti_{0.8})O_3$–$50(Ba_{0.7}Ca_{0.3})TiO_3$ Pb-free ceramic at the morphotropic phase boundary, Journal of Applied Physics 109 (2011) 054110.
[9] H.X. Bao, C. Zhou, D.Z. Xue, J.H. Gao, X.B. Ren (Eds.), Journal of Physics D: Applied Physics, 43, 2010, p. 465401.
[10] W.F. Liu, X.B. Ren, Large piezoelectric effect in Pb-free ceramics, Physical Review Letters 103 (2009) 257602–257604.
[11] X.S. Wang, H. Yamada, K. Nishikubo, C.N. Xu, Electrostrictive properties of Pr-doped $BaTiO_3$–$CaTiO_3$ ceramics, Japanese Journal of Applied Physics 45 (2006) 813–816.
[12] M.R. Panigrahi, S. Panigrahi, Structural analysis of 100% relative intense peak of $Ba_{1-x}Ca_xTiO_3$ ceramics by X-ray powder diffraction method, Physica B: Condensed Matter 405 (2010) 1787–1791.
[13] K. Uchino, Piezoelectric Actuators and Ultrasonic Motors, Kluwer Academic, Boston, 1997.
[14] R.E. Newnham, G.R. Ruschau, Smart electroceramics, Journal of the American Ceramic Society 74 (1991) 463.
[15] X.S. Wang, C.N. Xu, H. Yamada, K. Nishikubo, X.G. Zheng, Electro-mechano-optical conversions in Pr^{3+} doped $BaTiO_3$–$CaTiO_3$ ceramics, Advanced Materials 17 (2005) 1254–1258.
[16] L.F. Zhu, B.P. Zhang, W.G. Yang, N. Ma, X.K. Zhao, L. Zhao, High piezoelectric properties of (Ba,Ca)TiO3–0.04LiF ceramics sintered at a low temperature, Journal of Electroceramics 30 (2013) 24–29.
[17] H. Takahashi, Y. Numamoto, J. Tani, S. Tsurekawa, Piezoelectric properties of $BaTiO_3$ ceramics with high performance fabricated by microwave sintering, Japanese Journal of Applied Physics 45 (2006) 7405–7408.
[18] K. Tomoaki, Y. Kang, M. Toshiyuki, A. Masatoshi, Lead-free piezoelectric ceramics with large dielectric and piezoelectric constants manufactured from $BaTiO_3$ nano-powder, Japanese Journal of Applied Physics 46 (2007) 97–98.

[19] S.F. Shao, J.L. Zhang, Z. Zhang, P. Zheng, M.L. Zhao, J.C. Li, C.L. Wang, High piezoelectric properties and domain configuration in $BaTiO_3$ ceramics obtained through the solid-state reaction route, Journal of Physics D: Applied Physics 41 (2008) 125408.

[20] Z. Zhao, V. Buscaglia, M. Viviani, M.T. Buscaglia, L. Mitoseriu, A. Testino, M. Nygren, M. Johnsson, P. Nanni, Grain-size effects on the ferroelectric behavior of dense nanocrystalline $BaTiO_3$ ceramics, Physical Review B 70 (2004) 024107.

[21] S.W. Zhang, H.L. Zhang, B.P. Zhang, S. Yang, Phase-transition behavior and piezoelectric properties of lead-free $(Ba_{0.95}Ca_{0.05})(Ti_{1-x}Zr_x)O_3$ ceramics, Journal of Alloys and Compounds 506 (2010) 131–135.

[22] J. Zhi, Y. Zhi, A. Chen, Crystalline structure and dielectric properties of $Ba(Ti_{1-y}Ce_y)O_3$, Journal of Materials Science 38 (2003) 1057–1061.

[23] S. Mahajan, O.P. Thakur, D.K. Bhattacharya, K. Sreenivas, Ferroelectric relaxor behaviour and impedance spectroscopy of Bi_2O_3-doped barium zirconium titanate ceramics, Journal of Physics D: Applied Physics 42 (2009) 065413.

[24] G. Dividas, G. Prakash, Dielectric properties of A- and B-site doped $BaTiO_3$: effect of La and Ga, Physica B: Condensed Matter 404 (2009) 1799–1805.

[25] B. Xu, K.B. Yin, J. Lin, Y.D. Xia, X.G. Wan, J. Yin, X.J. Bai, J. Du, Z.G. Liu, Room-temperature ferromagnetism and ferroelectricity in Fe-doped $BaTiO_3$, Physical Review B 79 (2009) 134109.

[26] A. Watcharapasorn, S. Jiansirisomboon, T. Tunkasir, Sintering of Fe-doped $Bi_{0.5}Na_{0.5}TiO_3$ at $< 1000\,^{\circ}C$, Materials Letters 61 (2007) 2986–2989.

[27] A. Ullah, C.W. Ahn, S.Y. Lee, J.S. Kim, I.W. Kim, Structure, ferroelectric properties, and electric field-induced large strain in lead-free $Bi_{0.5}(Na,K)_{0.5}TiO_3$–$(Bi_{0.5}La_{0.5})AlO_3$ piezoelectric ceramics, Ceramics International. 38 (2012) 363–368.

[28] P.A. Jha, A.K. Jha, Influence of processing conditions on the grain growth and electrical properties of barium zirconate titanate ferroelectric ceramics, Journal of Alloys and Compounds 513 (2012) 580–585.